ELSEVIER

Journal of Nuclear Materials 290–293 (2001) 121–125

journal of nuclear materials

www.elsevier.nl/locate/jnucmat

Influence of oxygen on the carbide formation on tungsten

J. Luthin, Ch. Linsmeier *

Max-Planck-Institut für Plasmaphysik, EURATOM Association, Boltzmannstrasse 2, D-85748 Garching bei München, Germany

Abstract

As a first wall material in nuclear fusion devices, tungsten will interact with carbon and oxygen from the plasma. In this study, we report on the process of thermally induced carbide formation of thin carbon films on polycrystalline tungsten and the influence of oxygen on this process. All investigations are performed using X-ray photoelectron spectroscopy (XPS). Carbon films are supplied through electron beam evaporation of graphite. The carbidization process, monitored during increased substrate temperature, can be divided into four phases. In phase I disordered carbon converts into graphite-like carbon. In phase II significant diffusion and the reaction to W_2C is observed, followed by phase III which is dominated by the presence of W_2C and the beginning reaction to WC. Finally in phase IV only WC is present, but the total carbon amount has strongly decreased. Different mechanisms of oxygen influence on the carbide formation are proposed and measurements of the reaction of carbon on tungsten with intermediate oxide layers are presented in detail. A WO_{2+x} intermediate layer completely inhibits the carbide formation, while a WO_2 layer leads to WC formation at temperatures above 1270 K.

Keywords: Carbon; Carbon-based materials; Coating; Composite materials; Deposition; Erosion; First wall materials; High-*Z* material; Material mixing; Oxidation; Plasma facing materials; Thermal desorption; Tungsten; XPS

1. Introduction

The carbide formation on tungsten as one of the favorite materials for the plasma-facing components in current and future fusion experiments [1,2] is an issue of great importance as long as both elements tungsten and carbon are present at the first wall of the vacuum vessel [3]. Changes of the material properties occur after tungsten has formed a chemical compound. Deposition of carbon, which is e.g. eroded from graphite tiles used in addition to the tungsten components, can lead to the formation of W_2C and WC [4], depending on the conditions like supply of thermal energy or particle bombardment. Besides carbon, oxygen is one of the main impurities of a fusion plasma and present when a fusion experiment is not evacuated. Different reaction scenarios between tungsten, carbon and oxygen can be envisaged. We investigate the influence of oxygen on the carbon deposition and carbide formation on tungsten. After presenting the carbide formation process in the binary system W–C the adsorption and reactions of oxygen on tungsten are reported. Furthermore we focus on the temperature-dependant behavior of carbon films on tungsten with intermediate tungsten oxide layers of different oxidation states.

2. Experimental

All measurements are carried out in a PHI 5600 ESCA X-ray photoelectron spectroscopy (XPS) system which is equipped with a monochromatic Al Kα radiation source, a hemispherical energy analyzer, a sample heater (max. 970 K) and an ion gun (0.5–5.0 keV). The XPS system is connected to a preparation chamber where carbon films can be prepared by electron beam evaporation of graphite [4,5]. Certain O_2 partial pressures can be adjusted and O atoms can be created by an oxygen source using a microwave discharge [6,7]. In the preparation chamber annealing up to 1670 K is possible

* Corresponding author. Tel.: +49-89 3299 2285; fax: +49-89 3299 2279.

E-mail addresses: jens.luthin@ipp.mpg.de (J. Luthin), linsmeier@ipp.mpg.de (Ch. Linsmeier).

0022-3115/01/$ - see front matter
PII: S0022-3115(00)00429-3

by electron beam heating. Base pressures in both chambers are in the 10^{-8} Pa range. Details of the experimental setup are presented elsewhere [8]. For this investigation polycrystalline tungsten samples are used which do not show any contamination after combined sputter/annealing cycles (5.0 keV Ar^+/970 K). Carbon deposition provides pure films within the XPS detection sensitivity [4]. The WO_2 and WO_{2+x} oxide films are prepared in an external furnace under atmospheric conditions. To analyze the acquired XPS spectra curve fitting procedures were carried out using the MultiPak software package [9] and the Spectral Data Processor [10]. All spectra presented in this paper are shown after a Shirley background subtraction [11]. Binding energies are calibrated with respect to the Au $4f_{7/2}$ core level at 84.0 eV.

3. Results and discussion

3.1. Carbide formation

Thin carbon films are evaporated onto clean tungsten substrates at room temperature (RT, approx. 300 K) and a systematic study of the temperature-dependant reactions is performed by annealing the samples under UHV conditions. At each step the desired temperature was reached within 10 min and held for 30 min. We already reported the characterization of the deposited carbon films and first results of the carbide formation on tungsten [4]. During the annealing of the carbon layers on tungsten from 300 to 1670 K four phases can be discriminated. The carbon film of the annealing experiment shown in Fig. 1 has an initial thickness of 1.5 nm, calculated from the attenuation of the substrate photoelectrons [12,13]. The energy analyzer is operated at 2.95 eV pass energy to achieve high energy resolution which is especially necessary to interpret the 300 K carbon 1s spectra. After carbon deposition we find a peak in the W $4f_{7/2}$ spectrum located at 31.4 eV binding energy (BE) which is identified as elementary tungsten. In Fig. 1 the carbon 1s peaks are shown with the results of the curve fitting procedures. At 300 K the peak consists of two major contributions from elementary carbon. The signal at 284.2 eV originates from graphitic carbon, whereas the peak at 285.2 eV is attributed to a disordered carbon fraction [4]. From measurements of carbon layers in the submonolayer range we know that already at RT a small amount of carbide (BE 281.9 eV) is formed directly at the carbon–tungsten interface [14]. This is difficult to detect here due to the attenuation by the covering elementary carbon. Annealing steps up to 870 K lead to a conversion of the disordered carbon into graphitic carbon [4] which is the dominating process within phase I. The total amounts of carbon and tungsten stay constant within this temperature range. Recent time-dependant

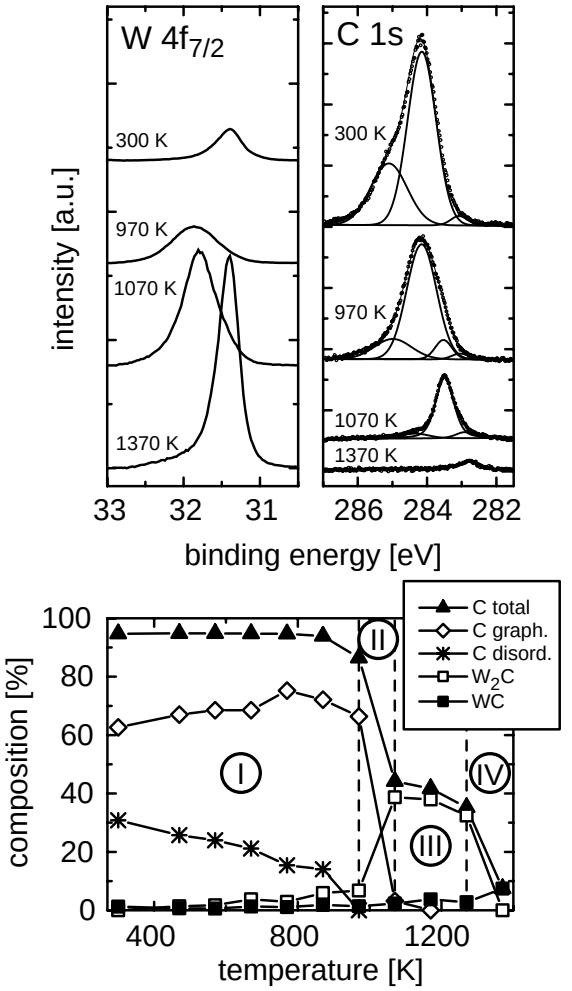

Fig. 1. W $4f_{7/2}$ and C 1s core level spectra and the surface layer composition of a carbon film on tungsten, monitored by XPS. Spectra are taken after annealing to the indicated temperatures. For the C 1s spectra the experimental data points are plotted as circles. The lines represent the peaks deconvoluted after fitting. The thin line beneath the data points is the sum of the deconvoluted peaks.

measurements have shown that diffusion below 870 K is very slow and increases significantly above this temperature [15]. This behavior is confirmed by simulations of carbon diffusion in tungsten [16]. The onset of phase II lies between 870 and 970 K. A part of the available carbon has reacted with the tungsten substrate to tungsten subcarbide (W_2C), indicated by a shift of 0.4 eV towards higher BE in the W $4f_{7/2}$ core level spectrum and a broadening of the C 1s peak. From that temperature on the amount of carbon is decreasing within the XPS detection depth and consequently that of tungsten is increasing. The C 1s spectrum recorded at 1070 K displays a shift of the peak maximum to 283.4 eV which agrees with the BE of W_2C. The W $4f_{7/2}$ spectrum has its

maximum at 31.8 eV with contributions of carbidic and metallic tungsten. At 1070 K we observe the transition between phases II and III of the carbidization process. Phase III is dominated by the presence of W_2C, which is formed by carbon atoms that occupy the octahedral sites of a hexagonal close-packed (hcp) W structure. Besides W_2C also WC can be found with a special WC structure, where the metal atoms form a hexagonal primitive packing and the carbon atoms are located in the middle of trigonal prisms built of tungsten atoms [17]. In phase III the reduction of the total carbon amount is slow compared to phase II. Above 1270 K (phase IV) we find the conversion of W_2C to WC which leads to a shift of the peak maximum in the C 1s region to 282.9 eV. This is accompanied by a further loss of carbon from the XPS analysis depth. The W $4f_{7/2}$ signal is shifted to 31.4 eV indicating that most of the intensity arises from elementary tungsten of the unreacted substrate. After all available carbon has reacted to WC, the process of carbide formation is complete.

3.2. Interaction with oxygen

An investigation of the ternary system C–O–W requires the consideration of various reaction paths. After presenting the process of carbide formation the interaction between oxygen and tungsten has to be discussed first. Many studies of oxygen adsorption on tungsten surfaces are reported which can be divided into different coverage ranges that are classified as chemisorption ($\leqslant 0.5$ monolayer (ML) oxygen coverage), two-dimensional oxidation (0.5–1.1 ML oxygen coverage) and bulk oxidation [18,19]. At RT exposure of tungsten to molecular oxygen results in dissociative chemisorption with oxygen atoms sitting at triply coordinated sites [20]. W $4f_{7/2}$ photoemission studies show that oxygen-induced features for $\leqslant 0.5$ ML oxygen coverage occur at $\sim$0.3 eV higher binding energies than the signal from bulk tungsten [21,22]. We measured polycrystalline tungsten samples after 5–60 min at 1×10^{-5} Pa O_2 partial pressure and after exposure to O atoms created in a microwave discharge [6]. In all cases we observe an oxygen coverage of $\sim$0.5 ML. The O 1s BE is located at 530.4 eV and the W 4f peaks are broadened. According to the literature, to achieve higher oxygen coverages the sample must be exposed either at elevated temperatures, for longer times or to higher oxygen pressures [23]. Annealing of the sample exposed 60 min at 1×10^{-5} Pa O_2 does not lead to changes in the tungsten/oxygen ratio up to 970 K. Above this temperature the oxygen amount decreases. However, after the last annealing to 1670 K an oxygen fraction of 10 at.% is still detected in the XPS signal. It is expected that atomic oxygen is the only desorption product for oxygen coverages below 0.5 ML [24]. With increasing coverage, a substantial part of oxygen can desorb as oxide [25]. We find that carbon deposition on chemisorbed oxygen and deposition of carbon in 1×10^{-5} Pa O_2 atmosphere with subsequent annealing do not reveal discrepancies in the process of carbide formation in the binary system W–C.

The influence of chemically bonded oxygen on the W–C interaction is studied at tungsten samples which are covered by thin oxide layers. Two different WO_x stoichiometries are examined. A WO_{2+x} with $x = 0.4$ is produced by annealing a sample (cleaned in vacuum as described above) in air for 60 min at 670 K. This treatment is carried out in a furnace under atmospheric conditions. The surface oxide exhibits a citric yellow color. After reinserting the sample into the UHV system XPS analysis results in a O/W ratio of 2.4 ($WO_{2.4}$). Annealing of the sample at 470 K for 10 min to remove volatile contaminations reduces the O/W ratio to 2.1. Since the substrate is pure W and the photoelectrons from W 4f have a higher kinetic energy than those from O 1s (1450 and 953 eV, respectively), the different attenuation lengths lead to an overestimation of the tungsten fraction in the O/W ratio. A $\sim$1 nm thick carbon layer is evaporated on this oxide layer. The XPS results after annealing steps up to 1670 K are presented in Fig. 2. At RT the W $4f_{7/2}$ BE is 35.7 eV. With decreasing oxidation state the BE decreases, literature values are 35.8 eV for WO_3 and 32.8 eV for WO_2 [26]. The peak maximum for O 1s is at 530.5 eV and for C 1s at 284.2 eV. Annealing to 970 K does not change the detected amounts of the three elements but a second W 4f doublet indicates that a part of the tungsten is reduced. In the O 1s energy range a shoulder at higher BE is detected. Further investigations are necessary to clarify the local stoichiometry of the oxide film, to elucidate the chemical state of the tungsten and to determine the structure of this oxide. Annealing to 1170 K leads to significant changes. The carbon signal disappears completely and the W $4f_{7/2}$ peak maximum shifts to 31.4 eV which indicates the presence of metallic tungsten. Dean et al. proposed a two-stage mechanism for the reduction of higher tungsten oxides with carbon via WO_2 to W under the formation of CO and CO_2 [27,28]. This mechanism is partly able to explain the reactions in our experiments. However, another reaction path is necessary which explains the decrease of the remaining oxygen without the presence of carbon above 1170 K. We like to emphasize that the 1670 K spectra are identical to the final state of the adsorption experiment of oxygen on clean tungsten.

To separate the two stages of the tungsten oxide reduction mechanism a second oxide stoichiometry – WO_2 – is examined. WO_2 films are prepared by annealing a cleaned tungsten substrate first at 820 K for 15 min in air (sample color: purple) and then at 970 K, 60 min under UHV conditions. XPS analysis showed an O/W ratio of less than 2 but for the reasons mentioned above the sample surface is assumed to be WO_2. This is also

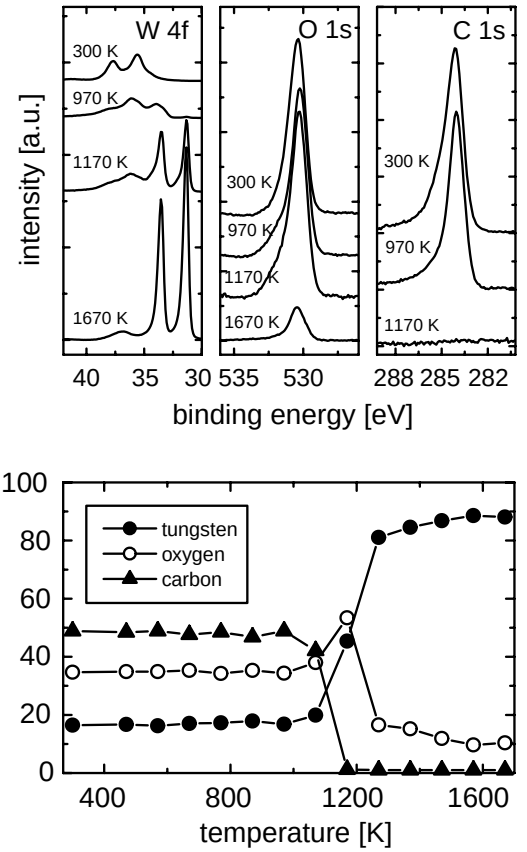

Fig. 2. XPS core level spectra and the surface layer composition as a function of the annealing temperature of a carbon film deposited on tungsten with a WO_{2+x} ($x = 0.4$) intermediate layer.

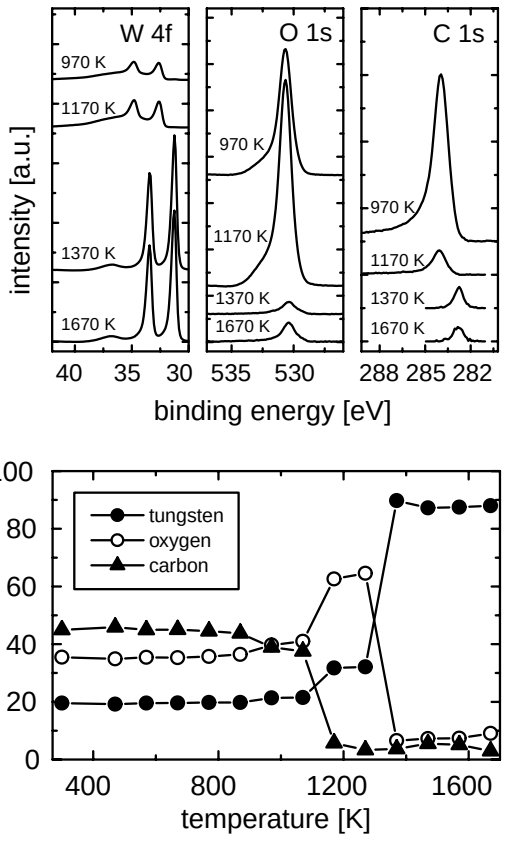

Fig. 3. XPS core level spectra and the surface layer composition as a function of the annealing temperature of a carbon film deposited on tungsten with a WO_2 intermediate layer.

confirmed by a W $4f_{7/2}$ BE of 32.8 eV, corresponding to the literature value. After carbon deposition annealing steps up to 970 K do not cause changes. Fig. 3 shows the XPS spectra and the surface composition during the subsequent annealing experiments. At 1170 K the tungsten is still present as WO_2, the carbon amount decreased again probably due to CO and CO_2 formation. However, in contrast to the $WO_{2.4}$ film, 6 at.% of graphitic carbon is left. The next annealing steps lead to a decrease in the oxygen amount but without a further decrease of the carbon intensity. Obviously, oxygen does not desorb from tungsten as a carbon compound at temperatures above 1170 K. We believe that the substitution $WO_2 \rightarrow WC$ is visible which is known for WO_2 reduction with CO [29,30]. At 1370 K all detectable carbon has completely reacted to WC indicated by a shift of the C 1s BE to 282.9 eV. Annealing to higher temperatures does not change the situation significantly. The final amount of oxygen is equal for all the other oxygen experiments. The reason for this similarity can be a very stable surface configuration at this oxygen concentration on tungsten.

4. Summary

We presented in detail the stepwise carbidization in the binary system W–C via W_2C to WC. An adsorbed oxygen layer or small amounts of oxygen during carbon film preparation on tungsten do not influence the process of carbide formation. However, intermediate oxide layers change the reaction behavior. A WO_{2+x} ($x = 0.4$) film inhibits the carbidization completely due to the reaction of carbon with oxygen. On a WO_2 layer carbon does not react with oxygen above 1170 K and with tungsten below 1370 K. At higher temperatures WC is formed without a W_2C subcarbide intermediate step. Further investigations will focus on the product spectrum and the mechanism of tungsten oxide reduction at temperatures above 1170 K. For the use of tungsten as first wall material in fusion devices we draw the conclusion that several reaction scenarios between W–O–C, depending on the initial conditions of the first wall, are

possible. This results in different surface layers with a broad variety of properties.

References

[1] J. Davis, V. Barabash, A. Makhankov, L. Plöchel, K. Slattery, J. Nucl. Mater. 258–263 (1998) 308.
[2] I. Kirillov, I. Danilov, S. Sidorenkov, Y. Strebkov, R. Mattas, Y. Gohar, T. Hua, D. Smith, Fusion Eng. Des. 39&40 (1998) 669.
[3] H. Maier, S. Kötterl, K. Krieger, R. Neu, M. Balden, ASDEX Upgrade-Team, J. Nucl. Mater. 258–263 (1998) 921.
[4] J. Luthin, Ch. Linsmeier, Surf. Sci. 454–456 (2000) 78.
[5] S. Schelz, T. Richmond, P. Kania, P. Oelhafen, H.-J. Güntherrodt, Surf. Sci. 359 (1996) 227.
[6] Ch. Linsmeier, J. Wanner, Surf. Sci. 454–456 (2000) 305.
[7] J. Jung, Max-Planck-Institut für Quantenoptik, MPQ-Report, 231, 1998.
[8] S. Miller, G. Berning, H. Plank, J. Roth, J. Vac. Sci. Technol. A 15 (1997) 2029.
[9] MultiPak Ver. 2.2, Physical Electronics, 1996.
[10] Spectral Data Processor, Ver. 2.1, XPS International, 1997.
[11] D. Shirley, Phys. Rev. B 5 (1972) 4709.
[12] M. Seah, Practical Surface Analysis, Wiley, Norwich, 1985.
[13] Ch. Linsmeier, Vacuum 6&7 (1994) 673.
[14] Ch. Linsmeier, J. Luthin, P. Goldstraß, these Proceedings.
[15] J. Luthin, K. Schmid, Ch. Linsmeier, J. Roth, to be published.
[16] K. Schmid, J. Roth, W. Eckstein, K. Ertl, these Proceedings.
[17] U. Müller, Anorganische Strukturchemie, Teubner, Stuttgart, 1992.
[18] T. Engel, H. Niehus, E. Bauer, Surf. Sci. 52 (1975) 237.
[19] E. Bauer, T. Engel, Surf. Sci. 71 (1978) 695.
[20] J. Feydt, A. Elbe, H. Egelhard, G. Meister, A. Goldmann, Surf. Sci. 440 (1999) 213.
[21] D.M. Riffe, G.K. Wertheim, Surf. Sci. 399 (1998) 248.
[22] C.H.F. Peden, N.D. Shin, Surf. Sci. 312 (1994) 151.
[23] H. Daimon, R. Ynzunza, J. Palomares, H. Takabi, C.S. Fadley, Surf. Sci. 408 (1998) 260.
[24] T. Engel, T. von dem Hagen, E. Bauer, Surf. Sci. 62 (1977) 361.
[25] D. Menzel, in: R. Gomer (Ed.), Topics in Applied Physics V.4. Interactions on Metal Surfaces, Berlin, 1975.
[26] J.F. Moulder, W.F. Strickle, P.E. Sobol, K.D. Bomben, in: J. Chastain (Ed.), Handbook of X-ray Photoelectron Spectroscopy, Perkin Elmer, MN, 1992.
[27] D.S. Venables, M.E. Brown, Thermochim. Acta 282&283 (1996) 251.
[28] D.S. Venables, M.E. Brown, Thermochim. Acta 282&283 (1996) 265.
[29] D.S. Venables, M.E. Brown, Thermochim. Acta 291 (1997) 131.
[30] T. Kodama, H. Ohtake, S. Matsumoto, A. Aoki, T. Shimizu, Y. Kitayama, Energy 25 (2000) 411.